

# Dynein light chain DLC-1 promotes localization and function of the PUF protein FBF-2 in germline progenitor cells

Xiaobo Wang<sup>1</sup>, Jenessa R. Olson<sup>1</sup>, Dominique Rasoloson<sup>2</sup>, Mary Ellenbecker<sup>1</sup>, Jessica Bailey<sup>1</sup> and Ekaterina Voronina<sup>1,\*</sup>

## ABSTRACT

PUF family translational repressors are conserved developmental regulators, but the molecular function provided by the regions flanking the PUF RNA-binding domain is unknown. In *C. elegans*, the PUF proteins FBF-1 and FBF-2 support germline progenitor maintenance by repressing production of meiotic proteins and use distinct mechanisms to repress their target mRNAs. We identify dynein light chain DLC-1 as an important regulator of FBF-2 function. DLC-1 directly binds to FBF-2 outside of the RNA-binding domain and promotes FBF-2 localization and function. By contrast, DLC-1 does not interact with FBF-1 and does not contribute to FBF-1 activity. Surprisingly, we find that the contribution of DLC-1 to FBF-2 activity is independent of the dynein motor. Our findings suggest that PUF protein localization and activity are mediated by sequences flanking the RNA-binding domain that bind specific molecular partners. Furthermore, these results identify a new role for DLC-1 in post-transcriptional regulation of gene expression.

**KEY WORDS:** Germline, Post-transcriptional regulation, RNA-binding protein, Stem cells, LC8 family proteins

## INTRODUCTION

Translational control is essential for numerous processes in development and learning, and it also impacts disease progression (Brinegar and Cooper, 2016). The PUF family of proteins is an important class of RNA-binding regulatory proteins that are conserved in most eukaryotes (Quenault et al., 2011). PUF family regulators promote translational repression and/or degradation of target mRNAs by directly binding conserved elements in the 3' untranslated region (UTR). PUF proteins often assemble with their target mRNAs and other translational regulators into RNA granules, cytoplasmic structures lacking a membrane boundary. For example, rat PUM2 and human PUM1 are found at stress granules, the sites of storage of translationally repressed mRNAs (Morris et al., 2008; Vessey et al., 2006).

To repress target mRNAs, PUF proteins are assembled in protein complexes with other co-regulator proteins (Miller and Olivas, 2011). The composition of PUF repressive complexes and the molecular mechanisms resulting in translational repression vary among organisms, tissue types and mRNA targets. Additionally, several negative regulators of PUF activity have been documented,

including a kinase that inhibits PUF activity by phosphorylation, as well as proteins that inhibit PUF protein-mRNA interactions (Miller and Olivas, 2011). Most known regulatory interactions involve the conserved PUF RNA-binding domain, despite the fact that the regions flanking the RNA-binding domain are required for full PUF activity (Muraro et al., 2008; Weidmann and Goldstrohm, 2012). There are no reports of PUF protein interactors that promote PUF subcellular localization or binding to the target mRNA.

In the germline of adult *Caenorhabditis elegans*, germ cells are arranged in a stereotypic progression, with stem cells located at the distal mitotic region and differentiating cells in a more proximal position (Pazdernik and Schedl, 2013). Cells displaced by division from the stem cell niche switch from proliferation to differentiation and enter meiosis, eventually forming differentiated gametes at the proximal end of the germline. *C. elegans* hermaphrodites produce sperm during late larval development and switch to oogenesis upon reaching adulthood. The balance between stem cell proliferation and differentiation supports stem cell maintenance and continued gamete production. Germline stem cell proliferation is regulated at the level of post-transcriptional control of gene expression (Kimble and Seidel, 2013). The regulatory network governing stem cell proliferation is closely integrated with the control of the switch from spermatogenesis to oogenesis (reviewed by Hansen and Schedl, 2013).


*C. elegans* germline stem cell maintenance depends on the activity of two conserved PUF family proteins, FBF-1 and FBF-2 (Zhang et al., 1997). In the absence of both FBF-1 and FBF-2, all cells in the mitotic zone precociously enter meiosis after the L4 stage of development when maintained at 20°C (Crittenden et al., 2002), but are maintained in a mitotic state if grown at 25°C (Merritt and Seydoux, 2010). FBF-1 and FBF-2 recognize the same motif present in the 3'UTR of their target mRNAs *in vitro* and form complexes with largely the same mRNAs *in vivo* (Bernstein et al., 2005; Merritt and Seydoux, 2010; Prasad et al., 2016). Despite high similarity between FBF-1 and FBF-2 (89% identity at the amino acid level) and apparent redundancy in their control of the switch from spermatogenesis to oogenesis, single *fbf-1* and *fbf-2* mutants have distinct phenotypes, suggesting that these genes play unique roles (Lamont et al., 2004). By examining the effects of single mutants on target mRNAs, it has been shown that FBF-1 inhibits accumulation of the target mRNAs in the mitotic zone and FBF-2 primarily represses mRNA translation (Voronina et al., 2012). In addition, only FBF-2 localizes to the germ cell-specific subtype of RNA granules called P granules, and this localization is required for the function of FBF-2 (Voronina et al., 2012). By contrast, FBF-1 does not localize to P granules and functions independently of these structures. The basis for these functional differences is not understood, but could involve interactions with distinct protein partners.

In this study, we report the identification of DLC-1 as a prominent regulator of FBF-2 localization and function. DLC-1 homologs

<sup>1</sup>Division of Biological Sciences, University of Montana, Missoula, MT 59812, USA.

<sup>2</sup>Department of Molecular Biology and Genetics, Johns Hopkins School of Medicine, HHMI, Baltimore, MD 21205, USA.

\*Author for correspondence (ekaterina.voronina@umontana.edu)

 E.V., 0000-0002-0194-4260

(known as LC8 family proteins) were first described as subunits of the cytoplasmic dynein motor complex that traffics organelles, proteins and RNAs towards microtubule minus ends (reviewed by Vale, 2003; Medioni et al., 2012; Roberts et al., 2013). More recently, LC8 proteins have emerged as ‘hub’ proteins that support assembly of protein complexes beyond the dynein motor (Rapali et al., 2011b). Direct DLC-1–FBF-2 interaction promotes FBF-2 localization to P granules and also promotes FBF-2 function. The DLC-1–FBF-2 complex functions in a dynein motor-independent manner. DLC-1 binds FBF-2 outside of the RNA-binding domain, and does not interact with FBF-1. Our work suggests that the regions flanking the FBF-2 RNA-binding PUF domain regulate FBF-2 localization through a specific molecular interaction. In addition, our results identify DLC-1 as a new player in post-transcriptional control of gene expression in development.

## RESULTS

### Identification of FBF-2-containing complexes

To identify novel protein co-factors important for FBF-mediated regulation in germline stem cells of *C. elegans*, we affinity purified FBF-2 protein complexes. We used anti-GFP antibodies to immunoprecipitate GFP::FBF-2 fusion protein expressed as a rescuing transgene in nematodes mutant for the endogenous *fbf-2* gene (Fig. S1A). To test whether any FBF-2 ribonucleoprotein complex components associate with FBF-2 in an RNA-dependent manner, we immunoprecipitated GFP::FBF-2 in the presence of RNase A (Fig. S1A,C), and analyzed both RNA-dependent and RNA-independent interactors. Proteins co-purifying with FBF-2 were identified by mass spectrometry. Among the proteins co-purified with FBF-2, many are RNA-binding proteins or splicing factors (Table 1). Other co-purifying proteins likely represent contaminants resulting from very high expression levels (for example, VIT-6/vitellogenin and UNC-54/myosin; Table S1). Four of the identified proteins were previously isolated with glutathione S-transferase (GST)-tagged FBF-2 from *C. elegans* lysates by GST pulldown (Friend et al., 2012). Proteins identified in negative controls (immunoprecipitations of GFP alone) or as abundant contaminants were excluded from consideration, leaving a smaller list of FBF-2-associated proteins; however, this approach does not guarantee that all contaminants were excluded (Mellacheruvu et al., 2013). Using this approach, we generated a list of candidate FBF-2 co-regulators for follow-up analysis (Table S1, genes tested by RNAi).

**Table 1. Proteins that co-purify with FBF-2 and are implicated in RNA regulation, cell signaling or intracellular trafficking**

Protein	Coverage (%)*	RNase sensitive?	Comment
FBF-2	42	No	Immunoprecipitation target
DLC-1	26	No	Dynein light chain
GLD-1	23	Yes	KH-domain RNA-binding protein
PAR-5	15	No	14-3-3 domain protein
CGH-1	12	Yes	DEAD-box helicase
DAZ-1	10	No	RNA-binding protein
RACK-1	9	Yes	Stress granule component
RSP-3	7	Yes	R/S rich, splicing factor
GLH-3	3	No	DEAD-box helicase, P granule component
CACN-1	3	Yes	Cactin, splicing factor

\*Calculated by dividing the number of amino acids in all peptides identified by mass spectrometry by the total number of amino acids in the entire protein sequence.

### A genetic screen identifies *dlc-1* as a potential co-regulator of *fbf-2*

We next performed a genetic screen to identify potential FBF-2 co-regulators inactivation of which causes synthetic enhancement of sterility in an *fbf-1* loss-of-function [abbreviated as *fbf-1(lf)*] background, compared with the wild-type and *fbf-2(lf)* backgrounds. Knockdown of the genes selectively required for FBF-2 function is expected to cause enhanced sterility when *fbf-1* is compromised, but not when FBF-1 is available to compensate for a disruption of FBF-2 activity. The knockdown experiments were performed in strains mutant for *rrf-1* to preferentially direct the effects of RNAi to the germline and avoid the indirect effects of depleting gene function in the somatic cells (Sijen et al., 2001; Kumsta and Hansen, 2012). These experiments focused on FBF-2 ribonucleoprotein (RNP) components with function related to RNA regulation, but included a number of other proteins identified in the co-immunoprecipitations. Out of knockdowns of 21 candidates, two, *dlc-1(RNAi)* and *rsp-3(RNAi)*, reproducibly showed increased sterility in the *fbf-1(lf)* background, but not in either wild-type or *fbf-2(lf)* backgrounds (Table S1). This study focuses on the investigation of the synthetic phenotype with the LC8-type dynein light chain *dlc-1*. Analysis of synthetic phenotypes with *rsp-3* was described elsewhere (Novak et al., 2015).

### DLC-1 contribution to FBF-2 function is independent of the dynein motor

DLC-1 was first described as an LC8-type subunit of the dynein motor complex (Pfister et al., 1982); however, extensive dynein-independent functions of DLC-1 have also been identified (Herzig et al., 2000; Rapali et al., 2011b). To investigate whether other components of the dynein motor complex contribute to FBF-2 activity, we tested for their genetic interaction with *fbf-1(lf)*. All 23 annotated *C. elegans* subunits of dynein and dynactin (dynein activity regulator and cargo adapter) complexes were depleted in *fbf-1(lf)* background and assayed for sterility (Fig. 1A). We find that only a single additional knockdown, dynein intermediate chain *dyci-1(RNAi)*, showed significantly increased sterility in the *fbf-1(lf)* background ( $P < 0.05$ , paired Student's *t*-test). Additionally, we found that RNAi of one of the dynein motor subunits, DHC-1, caused equally high sterility across the tested backgrounds (Fig. 1A,B). Knockdown of *dlc-1* is expected to disrupt both dynein-dependent and dynein-independent cellular functions; however, knockdowns of the other dynein complex subunits affect the motor function without disrupting motor-independent functions of DLC-1. The lack of genetic interactions between *fbf-1(lf)* and the majority of dynein motor subunits suggest that DLC-1 might promote the function of FBF-2 independently of the dynein motor.

We further tested whether FBF-2 function was affected in the genetic backgrounds with reduced *dhc-1* and *dlc-1* function using a hypomorphic temperature-sensitive (*ts*) mutation *dhc-1(or195)* and a deletion loss-of-function (*lf*) allele *dlc-1(tm3153)* (Hamill et al., 2002; this paper). We find that 78% of *fbf-1(lf); dlc-1(lf)* double mutants are sterile. This is a specific synthetic phenotype as 98% of *dlc-1(lf)* single mutants and *fbf-2(lf); dlc-1(lf)* double mutants are fertile and produce dead embryos (Table 2). By contrast, the *dhc-1(ts); fbf-1(lf)* double mutants grow to fertile adults when cultured from L1 larvae at the permissive temperature, and display similar penetrance of sterile adults and dead embryos at the restrictive temperature (Table 2). We conclude that *dlc-1*, but not *dhc-1*, shows significant genetic interaction with *fbf-1*, which is consistent with DLC-1 contributing to FBF-2 function.

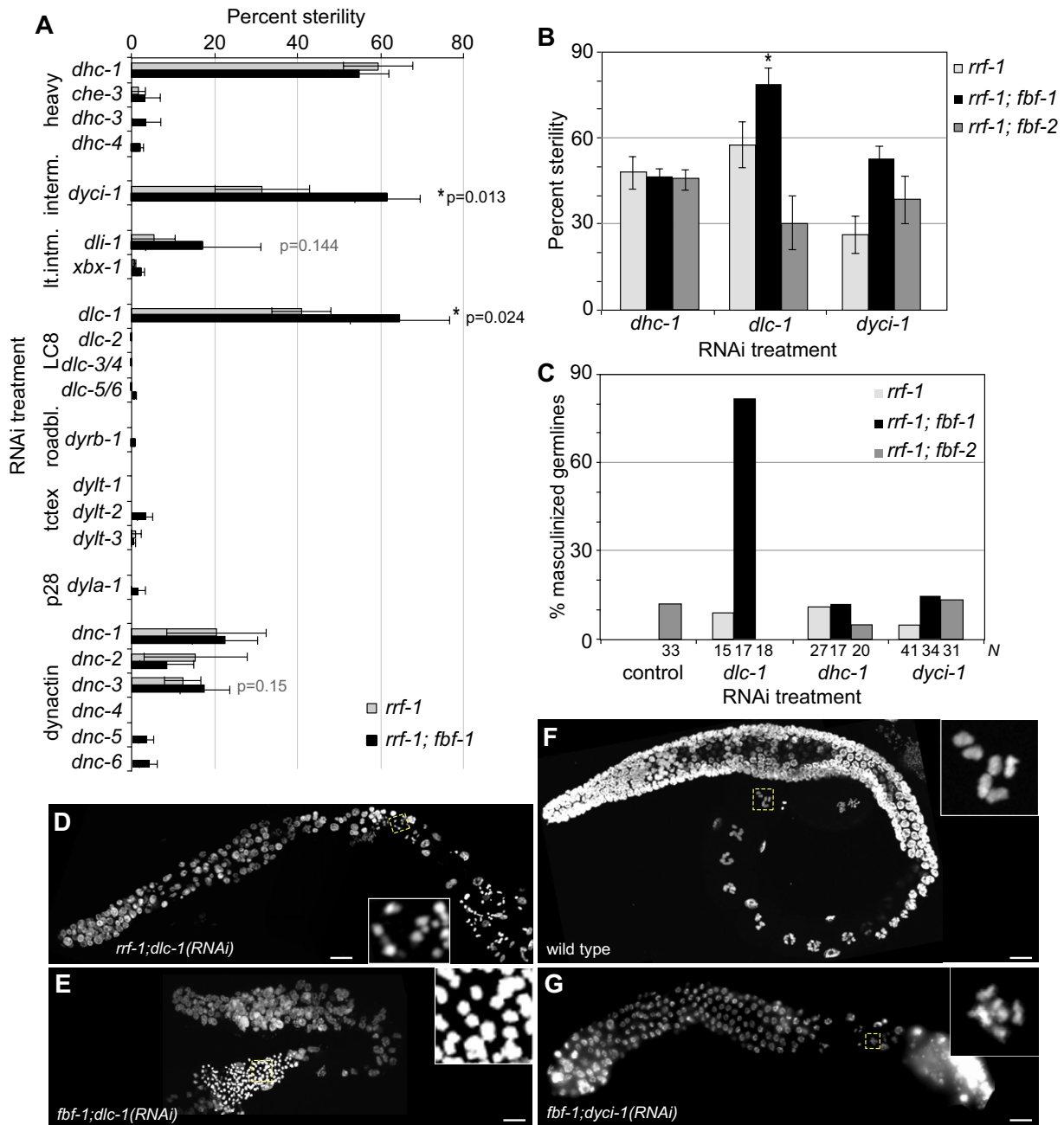


**Fig. 1. DLC-1 is required for FBF-2 function independent of the dynein motor complex.** (A) The percentage of sterile hermaphrodites in the *rrf-1* and *rrf-1; fbf-1* genetic backgrounds following RNAi treatments targeting various subunits of the dynein motor as indicated on the y-axis. Data are represented as mean  $\pm$  s.e.m. from three or four experiments scoring 25–60 worms per treatment. If a knockdown appeared to cause enhanced sterility in the *rrf-1; fbf-1* background, the differences between strains' response to that RNAi were evaluated for statistical significance by Student's paired *t*-test; *P* values are shown next to the treatment pairs, and significant differences are indicated by asterisks. (B) The percentage sterility in the *rrf-1*, *rrf-1; fbf-1* and *rrf-1; fbf-2* genetic backgrounds after the indicated RNAi treatments. Plotted are mean  $\pm$  s.e.m. from three or four experiments as in A. Asterisks mark the significant differences between genetic backgrounds in sterility caused by RNAi ( $P < 0.05$ ; corrected for multiple comparisons). The effects of each RNAi treatment on different strains were compared by one-way ANOVA [ $P < 0.001$  for *dlc-1(RNAi)*;  $P > 0.1$  for both *dhc-1* and *dyci-1(RNAi)*], followed by post-test comparison by Tukey's multiple comparison test. (C–F) Germline masculinization was observed after *dlc-1* knockdown. (C) Masculinization was scored after staining dissected gonads of sterile worms with DAPI 1 day post-L4 stage if formation of sperm but not oocytes was observed. The percentage of masculinized germlines is plotted for the *rrf-1*, *rrf-1; fbf-1* and *rrf-1; fbf-2* genetic backgrounds after the indicated RNAi treatments. Treatment of *rrf-1* and *rrf-1; fbf-1* mutants with control RNAi did not produce sterile worms. *n*, number of germlines scored (shown below the bars). (D) *rrf-1; dlc-1(RNAi)*, germline with small oocytes. (E) *fbf-1; dlc-1(RNAi)*, masculinized germline. (F) Control treatment, wild-type germline. (G) *fbf-1; dyci-1(RNAi)*, germline with degenerating endomitotic oocytes. Insets in D, F and G are magnified views of DAPI-stained oocyte chromatin. Inset in E shows magnified view of sperm chromatin. Regions enlarged in the insets are marked in panels D, F, G by dashed boxes. Scale bars: 10  $\mu$ m.

We next tested whether sterility observed after knockdown of three dynein subunits (*dlc-1*, *dhc-1* and *dyci-1*) resulted from the same defect as in *fbf-1 fbf-2* double mutants, which fail to initiate

oogenesis following initial spermatogenesis, resulting in masculinized germlines (Crittenden et al., 2002). By identifying chromatin morphology characteristic of spermatogenesis or

**Table 2. Synthetic sterility of *fbf-1*; *dlc-1* mutants**

Genotype and temperature	Sterile (%)*	<i>n</i>
<i>dlc-1(tm3153)</i> 20°C	2±2	156
<i>fbf-1(ok91); dlc-1(tm3153)</i> 20°C	78±12	231
<i>fbf-2(q738); dlc-1(tm3153)</i> 20°C	1±2	180
<i>dhc-1(or195); fbf-1(ok91)</i> 15°C	4±1 <sup>‡</sup>	181
<i>dhc-1(or195)</i> 15°C	5±1 <sup>‡</sup>	158
<i>dhc-1(or195); fbf-1(ok91)</i> 20°C	3±2	245
<i>dhc-1(or195)</i> 20°C	2±0.4	185
<i>dhc-1(or195); fbf-1(ok91)</i> 24°C	10±1	210
<i>dhc-1(or195)</i> 24°C	8±2	153

\*Sterile animals were identified by the absence of embryos in the uterus >24 h past the L4 larval stage, unless otherwise noted. Mean±s.d. shown. *n*, number of animals scored.

<sup>‡</sup>Animals grown at 15°C were analyzed 2 days post L4.

oogenesis, we find that sterility of *rrf-1*; *fbf-1* worms following *dlc-1(RNAi)* was associated with a significant degree of masculinization (Fig. 1C,E). By contrast, *dlc-1(RNAi)* in other genetic backgrounds and control RNAi in all backgrounds still allowed oocyte formation (Fig. 1C,D,F). Furthermore, we observed that masculinization was the cause of sterility observed in *fbf-1*; *dlc-1* double mutant animals (Table 3). Knockdowns of the other dynein components *dhc-1* and *dyci-1* in *rrf-1*; *rrf-1*; *fbf-1* and *rrf-1*; *fbf-2* backgrounds did not cause significant masculinization. The sterility in *dhc-1* and *dyci-1(RNAi)*-treated animals results from formation of small oocytes that became endomitotic (Fig. 1C,G). These results indicate that FBF-2 requires *dlc-1* and not *dhc-1* or *dyci-1* for function, and that FBF-1 does not require either of these.

Taken together, these results indicate that DLC-1 has a specific role in FBF-2 regulatory activity. As DLC-1 is the only subunit of the dynein motor that is required for FBF-2 function promoting oogenesis, we hypothesize that DLC-1 cooperation with FBF-2 is independent of the role of DLC-1 in the dynein motor complex. In the following experiments, we focus on testing the contribution of *dlc-1* to FBF-2-mediated regulation and include dynein motor subunit *dhc-1* knockdown to further substantiate the conclusion that the dynein motor does not affect FBF-2 function.

### DLC-1 is required for FBF-2-mediated RNA regulation

FBFs act as translational repressors by binding the 3'UTRs of their target mRNAs (Kimble and Seidel, 2013). We tested whether knockdown of *dlc-1* affected regulation of FBF target genes repressed in the mitotic region. *fog-1* is an FBF target that contains FBF regulatory sites in its 3'UTR (Thompson et al., 2005). A transgenic reporter, GFP::H2B::*fog-1* 3'UTR, recapitulates repression of *fog-1* in the distal cells and becomes derepressed in a *fbf-1 fbf-2* double mutant background (Merritt et al., 2008). Upon *dlc-1(RNAi)*, we observed derepression of the reporter in 54% of gonads of *fbf-1(lf)* mutant background, but not in the control genetic backgrounds (Fig. 2A,C). By contrast, *dhc-1(RNAi)* did not produce significant derepression in any genetic background, consistent with a dynein motor-independent role for DLC-1 in promoting FBF-2 function.

**Table 3. Masculinization of *fbf-1*; *dlc-1* mutant germlines**

Genotype	Masculinized (%)	<i>n</i>
<i>dlc-1(tm3153)</i>	0	27
<i>fbf-1(ok91); dlc-1(tm3153)</i>	89	28
<i>fbf-2(q738); dlc-1(tm3153)</i>	4	23

Animals were grown at 20°C, fixed and stained for gamete identification >24 h post L4 stage. *n*, number of animals scored.

HTP-1 and HTP-2 are two highly homologous HORMA domain meiotic proteins that are silenced by the FBFs in the mitotic region (Merritt and Seydoux, 2010). We observed ectopic expression of endogenous HTP-1 and HTP-2 in 87% of *dlc-1*; *fbf-1* hermaphrodites compared with 18% and 8% derepression in *dlc-1* and *dlc-1*; *fbf-2*, respectively (Fig. 2B,D). We conclude that *dlc-1*; *fbf-1* mutants display the same range of defects as observed in *fbf-1 fbf-2* mutants, consistent with conclusion that *dlc-1* is required for *fbf-2* activity.

### DLC-1 promotes FBF-2 localization to P granules

In the distal mitotic cells, FBF-2 is localized to perinuclear foci overlapping with P granules, and this localization is required for FBF-2 activity (Voronina et al., 2012). Because DLC-1 is required for FBF-2 regulatory activity, we tested whether DLC-1 played a role in FBF-2 localization to P granules. Using RNAi, we found that DLC-1 knockdown prevents FBF-2 localization to P granules in both wild-type and *fbf-1(lf)* backgrounds (Fig. 3A, first and second rows; Fig. S2A). By contrast, FBF-1 still localizes to perinuclear foci adjacent to but rarely overlapping with P granules (Fig. 3B; Fig. S2B,C). We found that FBF-2 protein levels are not affected by *dlc-1(RNAi)* (Fig. 3C). We conclude that DLC-1 is required to localize FBF-2 to P granules.

We next tested whether depletion of the dynein motor subunit DHC-1 or dynein intermediate chain DYCI-1 would affect FBF-2 protein localization. We found that following *dhc-1(RNAi)* or *dyci-1(RNAi)*, FBF-2 still localized to perinuclear P granules (Fig. 3A, third and fourth rows). The levels of FBF-2 protein were not affected by *dhc-1(RNAi)* (Fig. 3C). The effectiveness of *dhc-1(RNAi)* was verified by western blotting for endogenous DHC-1 (Fig. S2D). We conclude that FBF-2 localization to P granules does not depend on *dhc-1* or *dyci-1*.

### DLC-1 is broadly distributed in the cytoplasm and overlaps with P granules

If DLC-1 is involved with dynein motor-independent activities, the localization of DLC-1 is expected to be different from that of DHC-1. To compare the distribution of DLC-1 and DHC-1 proteins in the germline, we generated a single-copy FLAG-tagged transgene of DLC-1, which rescues *dlc-1(lf)*, and co-stained FLAG::DLC-1 with either endogenous DHC-1 (Gönczy et al., 1999) or the GFP::DHC-1 transgene (Gassmann et al., 2008). Both approaches yielded similar results. DHC-1 was observed, as previously reported, in perinuclear patches in the transition zone (Sato et al., 2009) and at the nuclear envelope in pachytene (Fig. 4A; Fig. S3A). By contrast, DLC-1 showed a broad diffuse distribution across the germline, overlapping with DHC-1, but without detectable enrichment at the sites of DHC-1 accumulation (Fig. 4A-C). We conclude that the differential localization of DLC-1 and DHC-1 supports the proposed motor-independent functions of DLC-1.

If DLC-1 is bound to FBF-2, a fraction of DLC-1 might be observed in P granules. Indeed, we find that FLAG::DLC-1 is present within P granules in both the mitotic region and the transition zone (Fig. 4B,C, insets). DLC-1 was not particularly enriched in P granules compared with overall cytoplasmic background. Additionally, we observed foci of DLC-1 that did not coincide with either P granules or DHC-1 patches. As DLC-1 overlaps with both P granules and DHC-1 patches, we conclude that DLC-1 might support function of both protein complexes.

To test whether DLC-1 localization to P granules depends on FBF-2 or dynein motor components, we documented DLC-1 localization

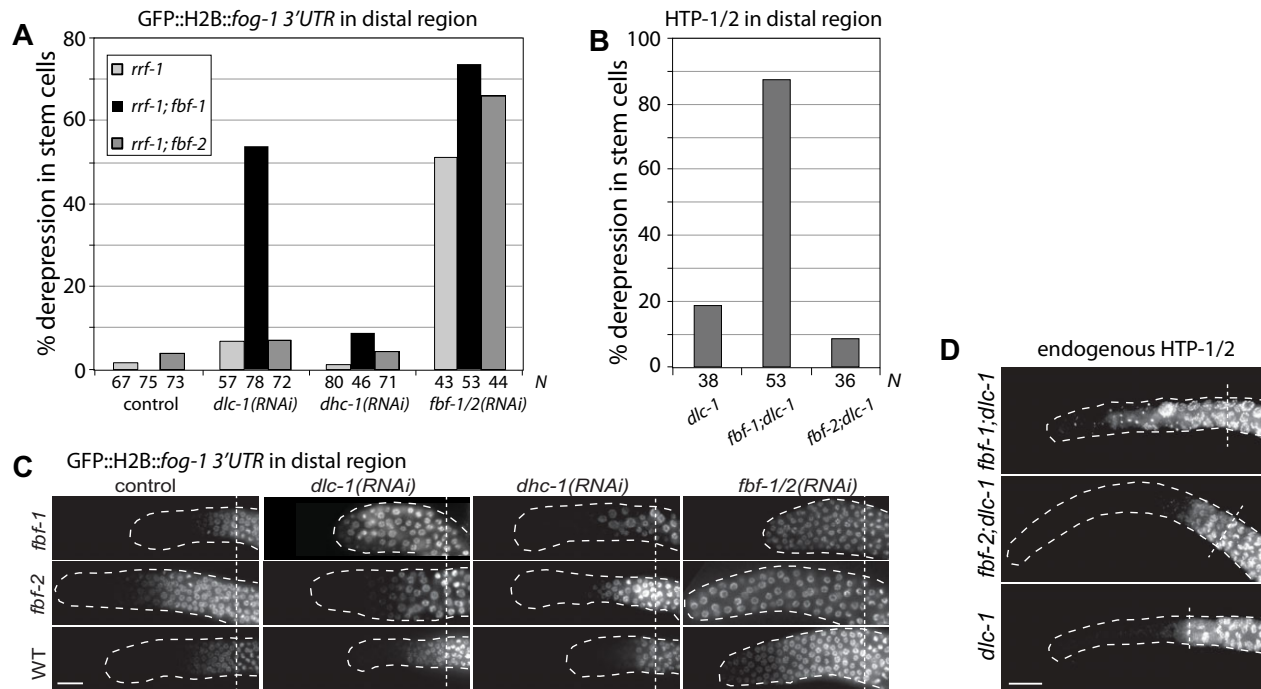


**Fig. 2. Knockdown of *dlc-1* affects FBF-2 regulatory function.** (A) The percentage of *rrf-1* (light gray), *rrf-1; fbf-1* (black) or *rrf-1; fbf-2* (dark gray) gonads following the indicated RNAi with GFP::H2B::*fog-1* 3'UTR expression extending to the distal end. *n*, number of germlines scored (shown below the bars). (B) The percentage of *dlc-1*, *fbf-1; dlc-1* and *fbf-2; dlc-1* gonads showing HTP-1/2 staining extending to the distal end. *n*, number of germlines scored (shown below the bars). (C) Distal gonads of the indicated genotypes expressing a GFP::Histone H2B fusion under the control of the *fog-1* 3'UTR after the indicated RNAi treatments. Gonads are outlined; vertical dashed lines indicate the beginning of the transition zone as recognized by the 'crescent-shaped' chromatin. All images were taken with a standard exposure. (D) Distal gonads of the indicated genotypes following *dlc-1*(RNAi) immunostained for the synaptonemal complex proteins HTP-1 and HTP-2 (the antibody recognizes both proteins; Martinez-Perez et al., 2008). Gonads are outlined; vertical dashed lines indicate the beginning of transition zone. Scale bars: 10  $\mu$ m.

following RNAi-mediated knockdown of FBFs, DHC-1 or DYCI-1. We find that DLC-1 overlaps P granules in all conditions tested, suggesting that DLC-1 localization to P granules is not affected by the dynein motor or the presence of FBF-2 (Fig. S3D).

### DLC-1 binds FBF-2 *in vitro*

To test whether the interaction between DLC-1 and FBF-2 is direct, we performed GST pulldown assays with recombinant GST-tagged DLC-1 and His-tagged FBF-2 and FBF-1. We found that His-tagged FBF-2, but not His-tagged FBF-1, binds GST-DLC-1 *in vitro* (Fig. 5A). FBF-1 and FBF-2 are highly similar, and their differences are focused in four 'variable regions', three of which map outside of the RNA-binding domain (Fig. 5B). We hypothesized that the interaction between FBF-2 and DLC-1 depends on the sequences in variable regions (VRs). To test which variable region(s) are important for FBF-2 binding to DLC-1, we created chimeric FBF-1 proteins, referred to as SWAP constructs, that contained a single FBF-2 variable region each (Fig. 5B). VR1, VR2 and VR4 of FBF-2 were each found to be sufficient to mediate interaction with DLC-1 when transferred to FBF-1 (Fig. 5C). LC8-type dynein light chains interact with linear peptide sequences of their direct targets that possess a relatively weak (D/S)KX(T/V/I)Q(T/V)(D/E) sequence motif; however, some interacting targets significantly deviate from this motif (Rapali et al., 2011a; Bodor et al., 2014). FBF-2 does not contain this sequence motif in the VRs mediating the interaction with DLC-1. We thus focused on the amino acids that differ between FBF-1 and FBF-2 in VR1 and VR2, and mutated them individually to identify the residues that contribute to the

interaction between FBF-2 and DLC-1 (Fig. S4A,B). Binding of FBF-2(VR1) to DLC-1 can be disrupted by a single mutation, P28A, and binding of FBF-2(VR2) to DLC-1 can be disrupted by either deleting Y139 and G140, or by mutating S136 and K137 to either asparagines (to imitate FBF-1) or alanines (Fig. S4B; X.W., unpublished). FBF-2(VR4) maps to the C-terminal tail, which is completely different from that of FBF-1. C-terminal truncation of VR4 by removing 26 amino acids completely prevents VR4 from binding DLC-1 (Fig. S4C). Combining these substitutions in VR1 and VR2 with the VR4 truncation in the context of the wild-type FBF-2 generated an FBF-2 mutant that was no longer able to bind DLC-1 *in vitro* (Fig. 5C). For simplicity, we refer to this mutant as FBF-2<sup>vmm</sup>.

We next tested whether the RNA-binding activity of FBF-2 was affected by the mutations that prevent the interaction with DLC-1. FBF-2 binding to RNA oligonucleotides with its recognition motif has been well characterized *in vitro* (Crittenden et al., 2002; Qiu et al., 2012). Typically, the FBF-2 RNA-binding domain is expressed and assayed in isolation, but as mutations in FBF-2<sup>vmm</sup> are all outside of the RNA-binding domain, we expressed full-length FBF-2<sup>wt</sup> and FBF-2<sup>vmm</sup> to characterize their binding to a fluorescently labeled target RNA oligonucleotide *in vitro*. Using fluorescence polarization, we found that FBF-2<sup>wt</sup> and FBF-2<sup>vmm</sup> bind to their target oligonucleotide with similar affinities (K<sub>d</sub> of 2.99  $\mu$ M and 2.91  $\mu$ M, respectively; Fig. 5D) that are not significantly different from one another ( $P=0.964$ ). We conclude that mutations preventing FBF-2 interaction with DLC-1 do not lead to general protein misfolding and do not affect FBF-2<sup>vmm</sup> RNA binding *in vitro*.

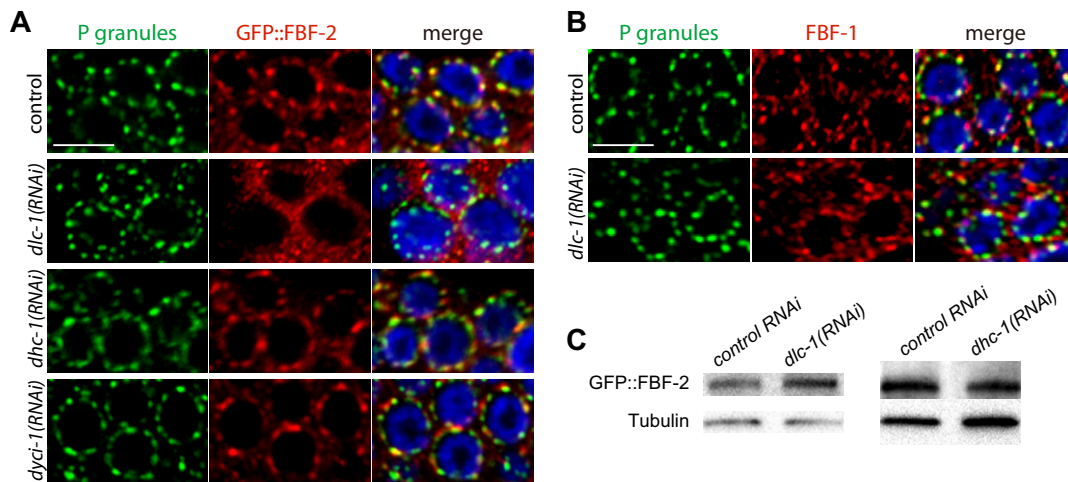


**Fig. 3. DLC-1 is required for FBF-2 localization.** (A,B) Confocal images of the mitotic zone of gonads following the indicated RNAi treatments double immunostained for the P granule component PGL-1 (green) and FBF-2 or FBF-1 (red). DNA is in blue. See also Fig. S2. Scale bars: 5  $\mu$ m. (C) Western blot of whole worm lysates following the indicated RNAi treatments. GFP::FBF-2 protein abundance does not decrease in the *dlc-1(RNAi)* or *dhc-1(RNAi)* backgrounds. Tubulin is used as a loading control.

#### Binding of DLC-1 is required for FBF-2 localization to perinuclear foci *in vivo*

To determine the effect of DLC-1 binding on FBF-2 localization *in vivo*, we generated a transgene expressing GFP::FBF-2<sup>vm</sup> and compared its localization in the germline with that of the wild-type GFP::FBF-2. As previously reported, wild-type GFP::FBF-2 localized to P granules in the distal cells (Fig. 6A). By contrast, GFP::FBF-2<sup>vm</sup>, which lacks the ability to interact with DLC-1, loses its enrichment in

perinuclear P granules (Fig. 6A) and localizes to cytoplasmic aggregates similar to wild-type GFP::FBF-2 in the absence of DLC-1 (Fig. 3A). We conclude that a direct interaction with DLC-1 is necessary for FBF-2 localization to perinuclear P granules.

#### Direct interaction with DLC-1 promotes FBF-2 function

P granule localization contributes to FBF-2 function (Voronina et al., 2012). Thus, we predict that FBF-2<sup>vm</sup> will show decreased

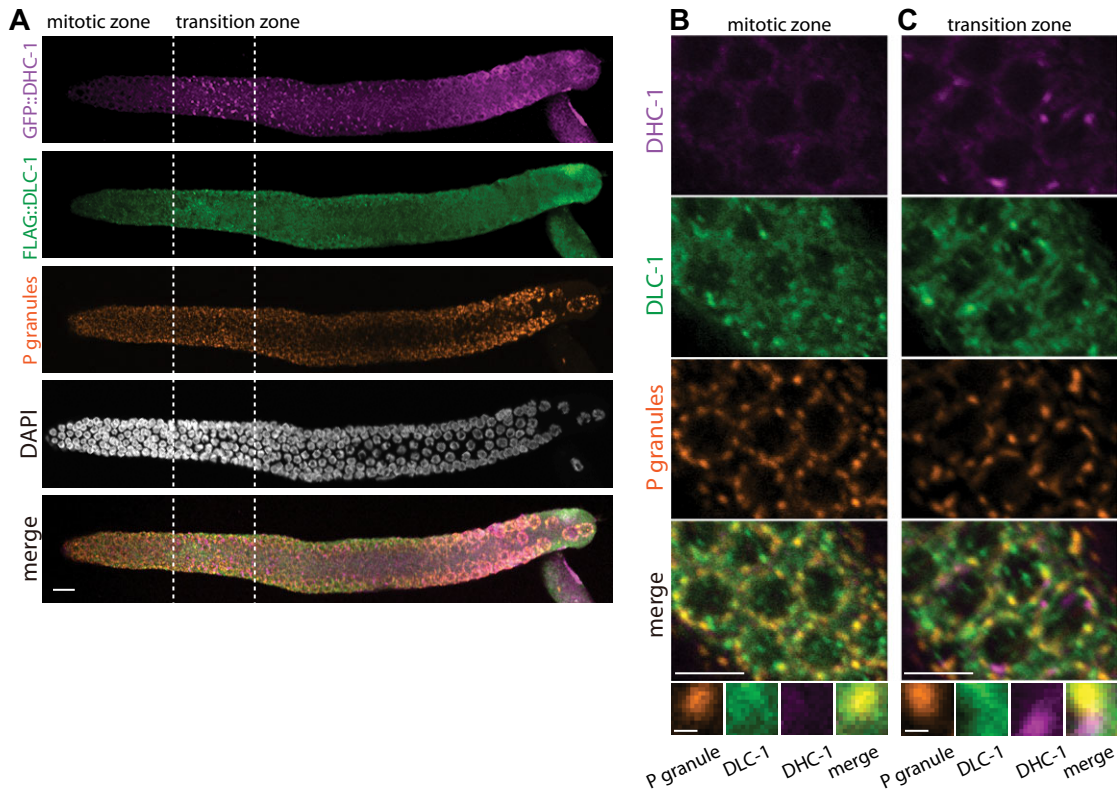


**Fig. 4. DLC-1 overlaps both P granules and DHC-1 patches.** (A) Expression of GFP::DHC-1 and FLAG::DLC-1 in a wild-type germ line. (B) In mitotic cells, FLAG::DLC-1 is broadly distributed and overlaps with P granules. A cropped image of a single P granule is shown below. (C) In meiotic cells (transition zone), FLAG::DLC-1 overlaps with both P granules and GFP::DHC-1 patches. GFP::DHC-1 patches do not colocalize with P granules. A cropped image of a P granule adjacent to a GFP::DHC-1 patch is shown below. Scale bars: 10  $\mu$ m (A); 5  $\mu$ m (B,C, top panels); 0.5  $\mu$ m (B,C, bottom cropped images).

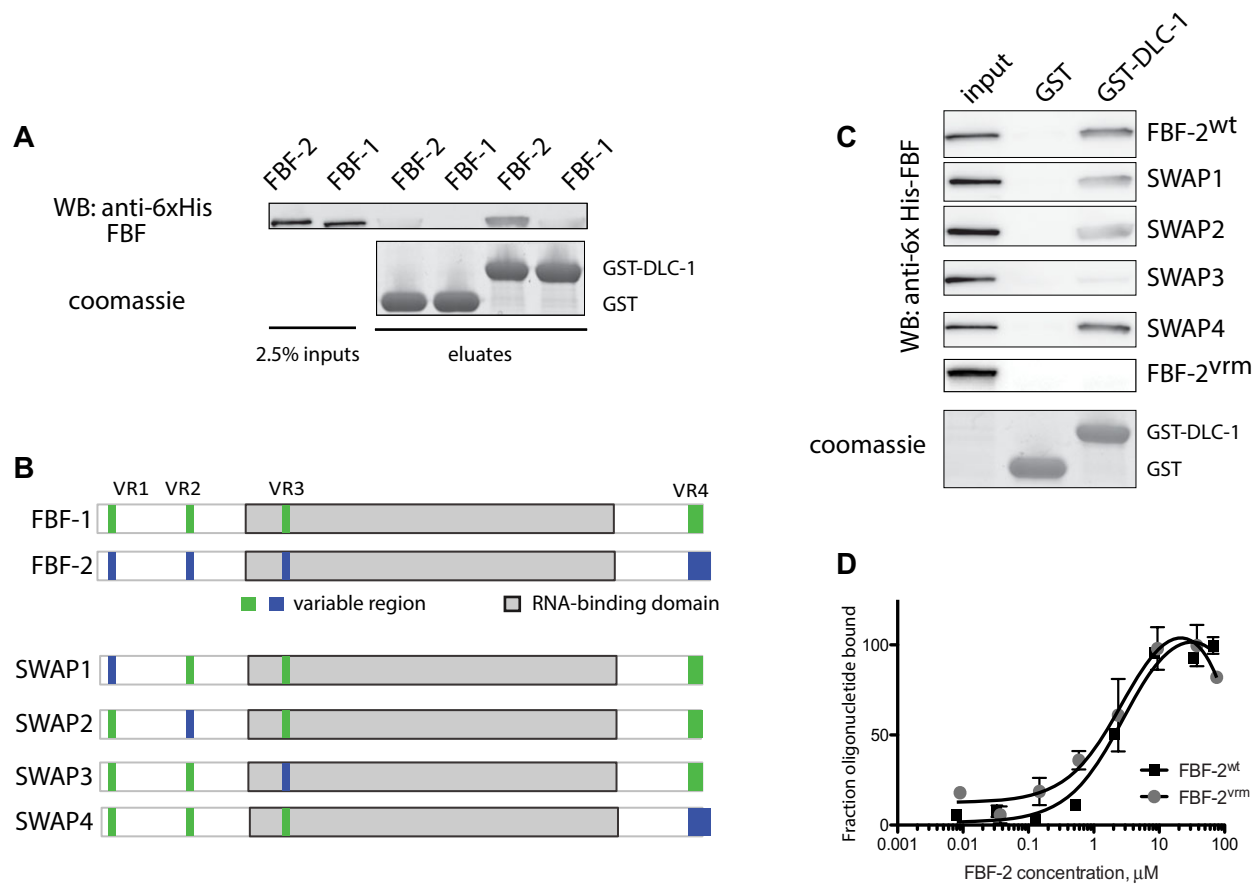


**Fig. 5. FBF-2 binds DLC-1 *in vitro*.** (A) GST-DLC-1 (Coomassie) was assayed for binding to full-length 6x-His-FBF-2 or 6x-His-FBF-1 (detected by western blotting). (B) Schematics of FBF-1 and FBF-2 proteins; variable regions 1–4 and RNA-binding domain are indicated. SWAP chimeric proteins were generated by transferring individual variable regions from FBF-2 to FBF-1. (C) Identification of the FBF-2 variable regions responsible for the interaction with DLC-1 using GST-pulldown analysis analogous to panel A. SWAP chimeric proteins are indicated on the right of the blots. FBF-2<sup>vr</sup> contains mutations in variable regions 1, 2 and 4 in the background of wild-type FBF-2 (P28A, S136A, K137A, deleted YG139–140, deleted amino acids 607–632). (D) FBF-2<sup>vr</sup> binds to the labeled oligonucleotide with the same affinity as the wild-type protein (K<sub>d</sub> of 2.99  $\mu\text{M}$  and 2.91  $\mu\text{M}$ , respectively;  $P=0.964$ ). Mean $\pm$ s.e.m. is shown.

ability to complement the genetic loss of *fbf-2*. As expected, a complementation assay showed that the GFP::FBF-2<sup>vr</sup> transgene exhibits a partial loss of function, and rescues the sterile *fbf-1 fbf-2* double mutant to fertility in 81% of the progeny. By contrast, wild-type GFP::FBF-2 rescues sterility of *fbf-1 fbf-2* double mutant in 97% of progeny (Table 4).

To test whether the DLC-1-binding regions are important in the context of the endogenous protein, we truncated 26 C-terminal amino acids from the endogenous *fbf-2* using CRISPR/Cas9. This mutation, designated *fbf-2(tr)*, removed one of the three DLC-1-binding sites and was generated in the *fbf-1* mutant background to allow functional analysis of the truncated FBF-2 without compensation by *fbf-1* function. We find that *fbf-1(lf) fbf-2(tr)* strains produce on average 11% sterile progeny when cultured at 24°C, suggesting that the truncated FBF-2 protein is not fully functional (Table 4). Chromatin staining of the sterile *fbf-1(lf) fbf-2(tr)* hermaphrodites indicates that sterility is due to a failure to initiate oogenesis during development, consistent with disruption of FBF function in the germline (Fig. 6B). Multiple DLC-1 binding sites might serve to increase overall affinity of FBF-2 for DLC-1 in a manner similar to other proteins with multiple LC8-binding motifs (Nyarko et al., 2013). We conclude that removing one of three DLC-1 binding sites affects FBF-2 activity *in vivo*.

#### Dynein motor-related DLC-1 function competes with FBF-2-related function

All data thus far indicate that DLC-1 functions with FBF-2 independently of its function with the dynein motor. To test further whether these functions are separable, we sought to determine whether the dynein motor and FBF-2 might compete for DLC-1 and thus antagonize each other. If true, release of DLC-1 from the dynein motor would be expected to result in enhanced motor-independent function of DLC-1. We took advantage of the partial loss of function of the *fbf-2(tr)* mutant, in which interaction of FBF-2(tr) with DLC-1 is weakened. If DLC-1 functions in a motor-independent manner, additional DLC-1 released from the dynein motor would promote more efficient FBF-2–DLC-1 complex formation and thus rescue FBF-2(tr) function and oocyte formation. By contrast, if FBF-2 requires dynein motor function, disruption of the motor by *dyci-1(RNAi)* should further compromise FBF-2(tr) function and enhance germline masculinization.

We released DLC-1 from the motor complex by knockdown of dynein intermediate chain *dyci-1*. Knockdown of *dyci-1* resulted in a significant decrease of germline masculinization compared with the control (Fig. 6C,D). This rescue of oocyte formation upon disruption of the motor complex, as opposed to enhancement of

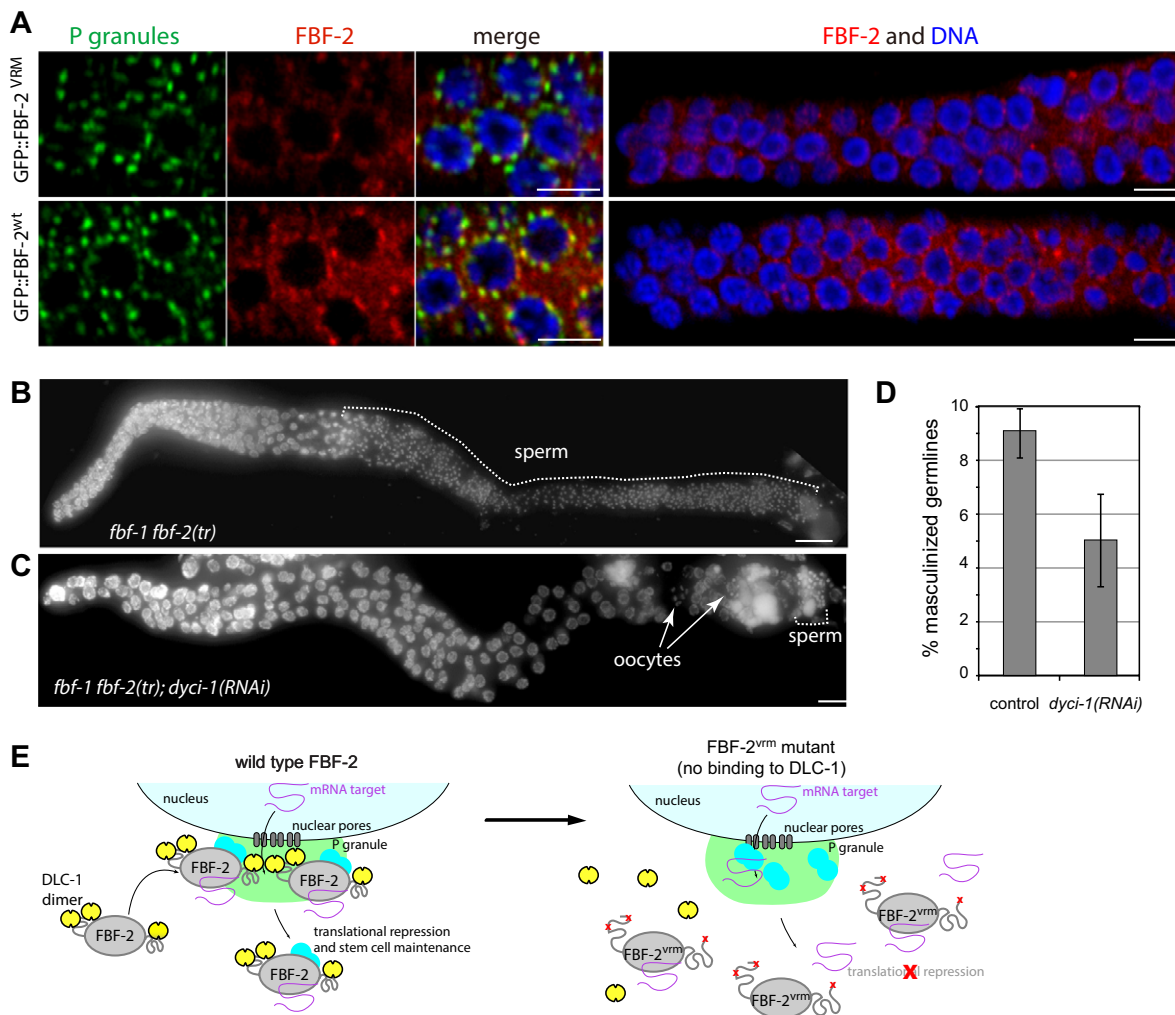


**Fig. 6. Interaction with DLC-1 is required for the localization and function of FBF-2 *in vivo*.** (A) Left panels: confocal images of GFP::FBF-2<sup>VRM</sup> and GFP::FBF-2<sup>wt</sup> expression in distal germ cells double immunostained with the antibodies to the P granule component PGL-1 (green) and to GFP (red). Right panels: lower-magnification confocal images of GFP::FBF-2<sup>VRM</sup> and GFP::FBF-2<sup>wt</sup> expression in the distal end of the germline immunostained for GFP (red); gonads are outlined. DNA is in blue. (B,C) Full gonads of sterile *fbf-1(f) fbf-2(tr)* mutants following control or *dyci-1(RNAi)* treatment stained with DAPI to reveal chromatin morphology. (B) Control germlines: excess sperm (dotted bracket) and no oogenesis. (C) *dyci-1(RNAi)*: small oocytes that become endomitotic. (D) Quantification of germline masculinization of *fbf-1(f) fbf-2(tr)* mutants following control or *dyci-1(RNAi)*. The average percentage of masculinization is significantly reduced in the *dyci-1(RNAi)* treatment compared with control ( $P < 0.01$  by Student's *t*-test). Mean  $\pm$  s.d. is shown. (E) Working model of DLC-1 supporting FBF-2 activity. Wild-type FBF-2 binds to DLC-1 via variable regions 1, 2 and 4. This binding promotes FBF-2 localization to P granules. Mutations in FBF-2 that preclude its association with DLC-1 interfere with FBF-2 localization to P granules and function. Scale bars: 5  $\mu$ m (A); 10  $\mu$ m (B,C).

masculinization, is consistent with DLC-1 functioning with FBF-2 independently of the dynein motor.

## DISCUSSION

This study supports three main conclusions that advance our understanding of PUF protein activity regulation. First, we reveal that the regions flanking the PUF RNA-binding domain regulate FBF-2 localization and activity through a specific interaction. Direct association of FBF-2 with DLC-1 is required for FBF-2 concentration in perinuclear P granules and promotes FBF-2 function (Fig. 6E). Second, by identifying and characterizing the first selective interacting partner of FBF-2 (versus FBF-1) we are able to improve our understanding of the basis for the observed differences between FBF-1/BBF-2 localization and regulatory activity. Third, our data show that the function of DLC-1 in promoting FBF-2 activity is independent of the role of DLC-1 in the dynein motor complex. Although dynein-independent functions of

DLC-1/LC8 proteins have been noted before, this study is the first report describing dynein-independent role of DLC-1/LC8 in post-transcriptional control of gene expression.

## Association with DLC-1 is required for FBF-2 localization

PUF proteins are conserved regulators of gene expression in development. Their core RNA-binding domain is required but not sufficient for translational repression (Deng et al., 2008; Muraro et al., 2008; Weidmann and Goldstrohm, 2012). *Drosophila* Pumilio and mammalian Pum2 have glutamine/asparagine-rich domains that might impact their association with RNA granules, but the mechanism of localization and its relevance to PUF activity are unclear (Vessey et al., 2006; Salazar et al., 2010). Our work identifies DLC-1 as the first molecular partner recruited through binding sites outside of the FBF-2 RNA-binding domain. Interaction with DLC-1 plays a crucial role in FBF-2 localization to perinuclear foci associated with P granules. DLC-1 does not



**Table 4. Transgenic rescue of *fbf-1 fbf-2* phenotypes and phenotype of *fbf-2(tr)* mutant in an *fbf-1* loss-of-function background**

	Sterile (%)	<i>n</i>
<i>fbf-1(lf) fbf-2(lf)+transgene</i>		
No transgene	100	61
<i>gfp::fbf-2(wt)</i>	3	90
<i>gfp::fbf-2(vrm)</i>	19	803
Genotype		
<i>fbf-1(lf)</i>	0	419
<i>fbf-1(lf) fbf-2(tr)</i> line 1	12	313
<i>fbf-1(lf) fbf-2(tr)</i> line 2	10	232

Sterility was scored under dissecting microscope by the absence of embryos in the uterus >24 h past the L4 larval stage at 24°C. *n*, number of animals scored.

appear to influence the stability of FBF-2 as DLC-1 knockdown does not affect FBF-2 protein levels.

How does association with DLC-1 change the spatial distribution of its binding partner? One possibility is that DLC-1 recruits FBF-2 to P granules by interacting with other P granule components. However, immunostaining indicates that DLC-1 overlaps with P granules, but is not enriched in P granules compared with the rest of the cytoplasm, suggesting that it is unlikely to target FBF-2 to P granules. An alternative is that DLC-1 forms a complex with FBF-2 in the cytoplasm, which then facilitates stabilization of the disordered regions of FBF-2, forming a scaffold for interaction with other protein partners to mediate recruitment to P granules. DLC-1 is expressed throughout the *C. elegans* germline (Dorsett and Schedl, 2009 and Fig. 4), with a broader distribution than the motor DHC-1, and is available to form a complex with FBF-2 in germline progenitor cells.

#### DLC-1 is an interactor specific for FBF-2

FBF-1 and FBF-2 are similar and partially redundant translational repressors important for *C. elegans* stem cell maintenance. Despite their sequence similarity and association with similar mRNA targets, FBF-1 and FBF-2 show distinct localization patterns in germ cells (Lamont et al., 2004; Voronina et al., 2012). Additionally, single mutants of *fbf-1* and *fbf-2* have opposite effects on the size of the mitotic region of the germline and distinct effects on their shared target mRNAs (Lamont et al., 2004; Voronina et al., 2012). These differences might be due to FBF-1 and FBF-2 interacting with distinct protein partners, and in this study we identify DLC-1 as the first interacting partner specific for FBF-2 over FBF-1. FBF-1 does not interact with DLC-1, and the localization and activity of FBF-1 are not affected by the presence of DLC-1. It is possible that FBF-1 assembles with its own specific binding partner(s) to facilitate its respective localization and function.

LC8 proteins associate with their partners through symmetrical binding sites formed at the two edges of the LC8 dimer interface and are able to interact with a diverse set of partner peptides (Barbar, 2008; Rapali et al., 2011b). LC8 binding motifs are short linear peptides, often found in intrinsically disordered segments. All three DLC-1-interacting motifs in FBF-2 are located outside of the well-structured RNA-binding domain and are predicted by the PrDOS algorithm to be disordered (Ishida and Kinoshita, 2007) at a 2% false-positive rate. The N-terminal DLC-1 binding sites are not well conserved in nematode FBF homologs. However, C-terminal extension found in FBF-2, but not FBF-1, is also present in the FBF-1/2 homologs from *Caenorhabditis japonica* and *briggsae*, suggesting that the interaction with DLC-1 might be conserved. Because none of these regions matches to a consensus DLC-1/LC8-

binding site, it would be informative improve our understanding of the structural basis of the FBF-2–DLC-1 association in the future.

#### DLC-1 promotes FBF-2 activity independent of the dynein motor

Cytoplasmic motors contribute to post-transcriptional regulation of gene expression. For example, the dynein motor complex is required for asymmetric RNP localization during *Drosophila* oogenesis and early embryogenesis (Wilkie and Davis, 2001; Bullock and Ish-Horowicz, 2001; Duncan and Warrior, 2002). Our results argue that DLC-1 contributes to FBF-2 function through a dynein motor-independent mechanism. The strongest evidence leading to this conclusion is that releasing DLC-1 from the dynein motor complex alleviates the phenotype of the truncated FBF-2(tr) lacking one of DLC-1 interaction sites. We hypothesize that DLC-1 promotes FBF-2 function by binding to FBF-2 and changing FBF-2 folding or assembly with other proteins.

#### DLC-1 as an allosteric regulator of protein function

LC8 proteins are highly conserved through evolution and contribute to a variety of biological processes (reviewed by Barbar, 2008). LC8 proteins function as regulatory hubs that promote assembly of protein complexes by interacting with short linear motifs of their binding partners (Rapali et al., 2011b). Structurally, binding of LC8 facilitates folding of its partners and increases their alpha-helical content (Nyarko et al., 2004; Bodor et al., 2014). The stabilized alpha-helices could then provide a binding interface for assembly of LC8 partners into larger protein complexes or otherwise allosterically modify their function. Further research is needed to elucidate whether FBF-2 association with DLC-1 changes FBF-2 structure or integration in a larger protein complex.

#### DLC-1 in RNA regulation

Is the dynein-independent contribution of DLC-1/LC8 to localization and function of RNA-binding proteins conserved? Similar to *C. elegans* FBF-2, the *Drosophila* RNA-binding protein Egalitarian (Egl), which is important for asymmetric RNP localization, binds the LC8 dynein light chain Dlc, and this association is required for Egl function (Navarro et al., 2004). Interestingly, a mutation in Egl that disrupts its binding to Dlc does not affect Egl association with the dynein motor adapter BicD. This Egl mutant might be tethered to the dynein motor yet non-functional (Navarro et al., 2004). Similar to FBF-2, the Egl mutant that is unable to bind Dlc can still associate with its RNA target *in vitro* (Dienstbier et al., 2009).

We propose that DLC-1/LC8 interactions with RNA-binding proteins might impact their regulatory output in a motor-independent fashion, analogous to what we observed for FBF-2. Our work adds post-transcriptional regulation of gene expression to the long list of LC8 functions. This finding opens new directions for further inquiry, such as what other RNA-binding proteins and mRNAs are found in association with DLC-1/LC8 and how association with DLC-1/LC8 affects regulatory activity of its partners.

#### MATERIALS AND METHODS

##### Nematode culture and genetics

*C. elegans* strains (Table S2) were derived from Bristol N2 and cultured as per standard protocols (Brenner, 1974) at 20°C or 24°C (if containing a transgene). FX14547 *dlc-1(tm3153)/hT2 III* was obtained from the National Bio-Resource Project (Japan), outcrossed to wild type, and rebalanced with a GFP-marked qC1 balancer to generate UMT222. *dlc-1(tm3153)*

results in a maternal-effect embryonic lethal phenotype. Homozygous *dlc-1(tm3153)* mutants produce both sperm and oocytes; however, oocytes in diakinesis have unpaired chromosomes similar to the *dlc-1(RNAi)* phenotype (Dorsett and Schedl, 2009; Fig. 1D) and result in dead embryos upon fertilization.

### Generation of transgenic and genetically modified animals

All transgene constructs were generated by Gateway cloning (Thermo Fisher Scientific); additional information is in the supplementary Materials and Methods. Transgene insertion into universal *Mos1* insertion sites was confirmed by PCR spanning homology region. The CRISPR/Cas9 co-conversion genome-editing approach (Arribere et al., 2014, Paix et al., 2014) was used to generate a 26-amino acid C-terminal deletion in endogenous *fbf-2*; mutants were identified by PCR genotyping screening and verified by restriction enzyme digest and Sanger sequencing. Two mutant lines generated by CRISPR/Cas9 approach were outcrossed six times with wild type before analysis.

### Immunolocalization and microscopy

Adult hermaphrodites were washed in M9 and germlines were dissected on poly-L-lysine treated slides, covered with a coverslip to ensure attachment to slide surface, and flash-frozen on aluminum blocks chilled on dry ice. The samples were fixed for 1 min in 100% methanol (−20°C) followed by 5 min in 2% electron microscopy-grade paraformaldehyde in 100 mM K<sub>2</sub>HPO<sub>4</sub> pH 7.2 at room temperature. The samples were blocked for at least 30 min in PBS/0.1% bovine serum albumin (BSA)/0.1% Tween 20. All primary antibody incubations were overnight at 4°C; all secondary antibody incubations were for 2 h at room temperature (antibodies are described in supplementary Materials and Methods).

### Imaging

Epifluorescence images were acquired with a Leica DFC3000G camera attached to a Leica DM5500B microscope with a 40× PL FLUOTAR NA1.3 objective using LAS-X software (Leica). Confocal images were obtained on Olympus FluoView FV1000 confocal mounted on an inverted IX81 microscope. Image processing was performed in Adobe Photoshop CS4.

### Immunoblotting

To determine the effect of *dlc-1(RNAi)* on FBF-2 levels, synchronized cultures of GFP::FBF-2(wt) were exposed to either *dlc-1* or control RNAi. Lysates were separated on 7.5% SDS-PAGE gels (Bio-Rad), and proteins were transferred to Immobilon-P PVDF membrane (EMD Millipore). After blocking in TBS/0.1% Tween 20/5% non-fat dry milk, the blots were probed with antibodies diluted in blocking solution. Antibodies are described in supplementary Materials and Methods. Blots were developed using Luminata Crescendo Western HRP substrate (EMD Millipore) and recorded on ChemiDoc MP Imaging System (Bio-Rad).

### Immunoprecipitation

Immunoprecipitation was performed as previously published (Voronina and Seydoux, 2010). The amount of proteins pulled down with and without RNase A treatment was compared by spectral counting label-free quantification (Bantscheff et al., 2007). See supplementary Materials and Methods for further details.

### RNAi

RNAi clones were either obtained from the Source BioScience RNAi library (Kamath and Ahringer, 2003) or generated by PCR amplification and cloning of genomic sequences into the pL4440 vector. Empty vector pL4440 was used as a control throughout the experiments. All plasmids were verified by sequencing and transformed into HT115(DE3) *Escherichia coli*. Three colonies of freshly transformed RNAi plasmids were combined for growth in LB/75 µg/ml carbenicillin media for 4 h, and induced with 10 mM isopropyl β-D-1-thiogalactopyranoside (IPTG) for 2 h at 37°C. RNAi plates (NNGM plates containing 75 µg/ml carbenicillin and 0.4 mM IPTG) were seeded with the pelleted cells. RNAi treatments were performed by feeding the L1 hermaphrodites synchronized by bleaching with bacteria expressing double-

stranded RNA for 3 days at 24°C. Sterility of the treated worms was scored when no embryos were observed in the uterus 1 day post L4. Masculinization of germlines was assessed after the treated worms were fixed and chromatin was stained with DAPI. Regulation of the GFP::H2B::*fog-1* 3'UTR reporter after RNAi was assessed by imaging dissected germlines (Novak et al., 2015).

### GST pulldown assay

For GST pulldown, cleared cell extracts of 6x-His-FBF proteins were added directly to GST-DLC-1 bound glutathione-Sepharose beads in 2 mM Tris pH 7.5, 500 mM NaCl, 10 mM beta-mercaptoethanol, 1 mg/ml BSA, 0.1% Triton X-100 and 1× protease inhibitor cocktail (Roche). Binding reactions were incubated at 15°C for 3 h and washed for four times with 10 mM Tris pH 7.5, 150 mM NaCl, 0.1% NP-40 and 1 mg/ml BSA. For elution, beads were heated to 80°C in sodium dodecyl sulfate sample buffer and 10 mM dithiothreitol. See supplementary Materials and Methods for details of recombinant protein production.

### Fluorescence polarization assay

Fluorescein-labeled RNA oligonucleotide [5'-(Flc)UCAUGGCCAUAC-3'; FBEa13; Qiu et al., 2012] was synthesized by Sigma-Aldrich. Polarization at each protein concentration was measured after incubation at room temperature for 40 min using a Biotek Synergy 2 plate reader, and dissociation constants were determined by GraphPad Prism. See supplementary Materials and Methods for further details, including recombinant protein production.

### Acknowledgements

We thank A. Dernburg and P. Gonczy for sharing antibodies; N. Day, M. Maley, E. Osterli and C. A. Pereira for assistance; G. Seydoux and A. Paix for protocols and reagents for co-CRISPR; E. Griffin, E. Gustafson and J. Wang for discussion. Several strains were provided by CGC funded by the NIH (P40 OD010440), and *dlc-1(tm3153)/hT2* was provided by National BioResource Project (Japan). The K76 antibody was obtained from the Developmental Studies Hybridoma Bank (NICH, The University of Iowa, Iowa City, IA, USA). We thank the University of Montana Molecular Histology and Fluorescence Imaging Core supported by P20RR017670 award from the NCRR.

### Competing interests

The authors declare no competing or financial interests.

### Author contributions

X.W., J.R.O., D.R., M.E., J.B., and E.V. performed experiments. X.W., J.R.O., M.E., and E.V. analyzed the data. E.V. conceived the study. X.W. and E.V. wrote the manuscript with comments from all authors.

### Funding

This work was supported by the National Institutes of Health (NIH) (GM109053 to E.V.), a University of Montana Research Award (to E.V.), and startup funds from a Center for Biomolecular Structure and Dynamics NIH CoBRE grant (P20GM103546 to E.V.). Deposited in PMC for release after 12 months.

### Supplementary information

Supplementary information available online at <http://dev.biologists.org/lookup/doi/10.1242/dev.140921.supplemental>

### References

- Arribere, J. A., Bell, R. T., Fu, B. X., Artilles, K. L., Hartman, P. S. and Fire, A. Z. (2014). Efficient marker-free recovery of custom genetic modifications with CRISPR/Cas9 in *Caenorhabditis elegans*. *Genetics* **198**, 837–846.
- Bantscheff, M., Schirle, M., Sweetman, G., Rick, J. and Kuster, B. (2007). Quantitative mass spectrometry in proteomics: a critical review. *Anal. Bioanal. Chem.* **389**, 1017–1031.
- Barbar, E. (2008). Dynein light chain LC8 is a dimerization hub essential in diverse protein networks. *Biochemistry* **47**, 503–508.
- Bernstein, D., Hook, B., Hajarnavis, A., Opperman, L. and Wickens, M. (2005). Binding specificity and mRNA targets of a *C. elegans* PUF protein, FBF-1. *RNA* **11**, 447–458.
- Bodor, A., Radnai, L., Hetényi, C., Rapali, P., Láng, A., Kövér, K. E., Perczel, A., Wahlgren, W. Y., Katona, G. and Nyitray, L. (2014). DYNLL2 dynein light chain binds to an extended linear motif of myosin 5a tail that has structural plasticity. *Biochemistry* **53**, 7107–7122.
- Brenner, S. (1974). The genetics of *Caenorhabditis elegans*. *Genetics* **77**, 71–94.

- Brinegar, A. E. and Cooper, T. A.** (2016). Roles for RNA-binding proteins in development and disease. *Brain Res.* **1647**, 1–8.
- Bullock, S. L. and Ish-Horowitz, D.** (2001). Conserved signals and machinery for RNA transport in *Drosophila* oogenesis and embryogenesis. *Nature* **414**, 611–616.
- Crittenden, S. L., Bernstein, D. S., Bachorik, J. L., Thompson, B. E., Gallegos, M., Petcherski, A. G., Moulder, G., Barstead, R., Wickens, M. and Kimble, J.** (2002). A conserved RNA-binding protein controls germline stem cells in *Caenorhabditis elegans*. *Nature* **417**, 660–663.
- Deng, Y., Singer, R. H. and Gu, W.** (2008). Translation of ASH1 mRNA is repressed by Puf6p-Fun12p/eIF5B interaction and released by CK2 phosphorylation. *Genes Dev.* **22**, 1037–1050.
- Dienstbier, M., Boehl, F., Li, X. and Bullock, S. L.** (2009). Egalitarian is a selective RNA-binding protein linking mRNA localization signals to the dynein motor. *Genes Dev.* **23**, 1546–1558.
- Dorsett, M. and Schedl, T.** (2009). A role for dynein in the inhibition of germ cell proliferative fate. *Mol. Cell. Biol.* **29**, 6128–6139.
- Duncan, J. E. and Warrior, R.** (2002). The cytoplasmic dynein and kinesin motors have interdependent roles in patterning the *Drosophila* oocyte. *Curr. Biol.* **12**, 1982–1991.
- Friend, K., Campbell, Z. T., Cooke, A., Kroll-Conner, P., Wickens, M. P. and Kimble, J.** (2012). A conserved PUF-Ago-eEF1A complex attenuates translation elongation. *Nat. Struct. Mol. Biol.* **19**, 176–183.
- Gassmann, R., Essex, A., Hu, J.-S., Maddox, P. S., Motegi, F., Sugimoto, A., O'Rourke, S. M., Bowerman, B., McLeod, I., Yates, J. R. et al.** (2008). A new mechanism controlling kinetochore-microtubule interactions revealed by comparison of two dynein-targeting components: SPDL-1 and the Rod/Zw10/Zw10 complex. *Genes Dev.* **22**, 2385–2399.
- Gönczy, P., Pichler, S., Kirkham, M. and Hyman, A. A.** (1999). Cytoplasmic dynein is required for distinct aspects of MTOC positioning, including centrosome separation, in the one cell stage *Caenorhabditis elegans* embryo. *J. Cell Biol.* **147**, 135–150.
- Hamill, D. R., Severson, A. F., Carter, J. C. and Bowerman, B.** (2002). Centrosome maturation and mitotic spindle assembly in *C. elegans* require SPD-5, a protein with multiple coiled-coil domains. *Dev. Cell* **3**, 673–684.
- Hansen, D. and Schedl, T.** (2013). Stem cell proliferation versus meiotic fate decision in *Caenorhabditis elegans*. *Adv. Exp. Med. Biol.* **757**, 71–99.
- Herzig, R. P., Andersson, U. and Scarpulla, R. C.** (2000). Dynein light chain interacts with NRF-1 and EWG, structurally and functionally related transcription factors from humans and *Drosophila*. *J. Cell Sci.* **113**, 4263–4273.
- Ishida, T. and Kinoshita, K.** (2007). PrDOS: prediction of disordered protein regions from amino acid sequence. *Nucleic Acids Res.* **35**, W460–W464.
- Kamath, R. S. and Ahringer, J.** (2003) Genome-wide RNAi screening in *Caenorhabditis elegans*. *Methods* **30**, 313–321.
- Kimble, J. and Seidel, H.** (2013). *C. elegans* germline stem cells and their niche. In *StemBook* (ed. The Stem Cell Research Community), doi/10.3824/stembook.1.95.1.
- Kumsta, C. and Hansen, M.** (2012). *C. elegans* rrf-1 mutations maintain RNAi efficiency in the soma in addition to the germline. *PLoS ONE* **7**, e35428.
- Lamont, L. B., Crittenden, S. L., Bernstein, D., Wickens, M. and Kimble, J.** (2004). FBF-1 and FBF-2 regulate the size of the mitotic region in the *C. elegans* germline. *Dev. Cell* **7**, 697–707.
- Martinez-Perez, E., Schvarzstein, M., Barroso, C., Lightfoot, J., Dernburg, A. F. and Villeneuve, A. M.** (2008). Crossovers trigger a remodeling of meiotic chromosome axis composition that is linked to two-step loss of sister chromatid cohesion. *Genes Dev.* **22**, 2886–2901.
- Medioni, C., Mowry, K. and Besse, F.** (2012). Principles and roles of mRNA localization in animal development. *Development* **139**, 3263–3276.
- Mellacheruvu, D., Wright, Z., Couzens, A. L., Lambert, J.-P., St-Denis, N. A., Li, T., Miteva, Y. V., Hauri, S., Sardi, M. E., Low, T. Y. et al.** (2013). The CRAPome: a contaminant repository for affinity purification-mass spectrometry data. *Nat. Methods* **10**, 730–736.
- Merritt, C. and Seydoux, G.** (2010). The Puf RNA-binding proteins FBF-1 and FBF-2 inhibit the expression of synaptonemal complex proteins in germline stem cells. *Development* **137**, 1787–1798.
- Merritt, C., Rasoloson, D., Ko, D. and Seydoux, G.** (2008). 3 UTRs are the primary regulators of gene expression in the *C. elegans* germline. *Curr. Biol.* **18**, 1476–1482.
- Miller, M. A. and Olivias, W. M.** (2011). Roles of Puf proteins in mRNA degradation and translation. *Wiley Interdiscip. Rev. RNA* **2**, 471–492.
- Morris, A. R., Mukherjee, N. and Keene, J. D.** (2008). Ribonomic analysis of human Pum1 reveals cis-trans conservation across species despite evolution of diverse mRNA target sets. *Mol. Cell. Biol.* **28**, 4093–4103.
- Muraro, N. I., Weston, A. J., Gerber, A. P., Luschnig, S., Moffat, K. G. and Baines, R. A.** (2008). Pumilio binds para mRNA and requires Nanos and Brat to regulate sodium current in *Drosophila* motoneurons. *J. Neurosci.* **28**, 2099–2109.
- Navarro, C., Puthalakath, H., Adams, J. M., Strasser, A. and Lehmann, R.** (2004). Egalitarian binds dynein light chain to establish oocyte polarity and maintain oocyte fate. *Nat. Cell Biol.* **6**, 427–435.
- Novak, P., Wang, X., Ellenbecker, M., Feilzer, S. and Voronina, E.** (2015). Splicing machinery facilitates post-transcriptional regulation by FBFs and other RNA-binding proteins in *Caenorhabditis elegans* Germline. *G3 (Bethesda)* **5**, 2051–2059.
- Nyarko, A., Hare, M., Hays, T. S. and Barbar, E.** (2004). The intermediate chain of cytoplasmic dynein is partially disordered and gains structure upon binding to light-chain LC8. *Biochemistry* **43**, 15595–15603.
- Nyarko, A., Song, Y., Nováček, J., Židek, L. and Barbar, E.** (2013). Multiple recognition motifs in nucleoporin Nup159 provide a stable and rigid Nup159-Dyn2 assembly. *J. Biol. Chem.* **288**, 2614–2622.
- Paix, A., Wang, Y., Smith, H. E., Lee, C. Y., Calidas, D., Lu, T., Smith, J., Schmidt, H., Krause, M. W. and Seydoux, G.** (2014). Scalable and versatile genome editing using linear DNAs with microhomology to Cas9 Sites in *Caenorhabditis elegans*. *Genetics* **198**, 1347–1356.
- Pazdernik, N. and Schedl, T.** (2013). Introduction to germ cell development in *Caenorhabditis elegans*. *Adv. Exp. Med. Biol.* **757**, 1–16.
- Pfister, K. K., Fay, R. B. and Witman, G. B.** (1982). Purification and polypeptide composition of dynein ATPases from *Chlamydomonas* flagella. *Cell Motil.* **2**, 525–547.
- Prasad, A., Porter, D. F., Kroll-Conner, P. L., Mohanty, I., Ryan, A. R., Crittenden, S. L., Wickens, M. and Kimble, J.** (2016). The PUF binding landscape in metazoan germ cells. *RNA* **22**, 1026–1043.
- Qiu, C., Kershner, A., Wang, Y., Holley, C. P., Wilinski, D., Keles, S., Kimble, J., Wickens, M. and Hall, T. M. T.** (2012). Divergence of Pumilio/fem-3 mRNA binding factor (PUF) protein specificity through variations in an RNA-binding pocket. *J. Biol. Chem.* **287**, 6949–6957.
- Quenault, T., Lithgow, T. and Travençolo, A.** (2011). PUF proteins: repression, activation and mRNA localization. *Trends Cell Biol.* **21**, 104–112.
- Rapali, P., Radnai, L., Süveges, D., Harmat, V., Tölgyesi, F., Wahlgren, W. Y., Katona, G., Nyitray, L. and Pál, G.** (2011a). Directed evolution reveals the binding motif preference of the LC8/DYNLL hub protein and predicts large numbers of novel binders in the human proteome. *PLoS ONE* **6**, e18818.
- Rapali, P., Szenes, Á., Radnai, L., Bakos, A., Pál, G. and Nyitray, L.** (2011b). DYNLL/LC8: a light chain subunit of the dynein motor complex and beyond. *FEBS J.* **278**, 2980–2996.
- Roberts, A. J., Kon, T., Knight, P. J., Sutoh, K. and Burgess, S. A.** (2013). Functions and mechanics of dynein motor proteins. *Nat. Rev. Mol. Cell Biol.* **14**, 713–726.
- Salazar, A. M., Silverman, E. J., Menon, K. P. and Zinn, K.** (2010). Regulation of synaptic Pumilio function by an aggregation-prone domain. *J. Neurosci.* **30**, 515–522.
- Sato, A., Isaac, B., Phillips, C. M., Rillo, R., Carlton, P. M., Wynne, D. J., Kasad, R. A. and Dernburg, A. F.** (2009). Cytoskeletal forces span the nuclear envelope to coordinate meiotic chromosome pairing and synapsis. *Cell* **139**, 907–919.
- Sijen, T., Fleenor, J., Simmer, F., Thijssen, K. L., Parrish, S., Timmons, L., Plasterk, R. H. A. and Fire, A.** (2001). On the role of RNA amplification in dsRNA-triggered gene silencing. *Cell* **107**, 465–476.
- Thompson, B. E., Bernstein, D. S., Bachorik, J. L., Petcherski, A. G., Wickens, M. and Kimble, J.** (2005). Dose-dependent control of proliferation and sperm specification by FOG-1/CPEB. *Development* **132**, 3471–3481.
- Vale, R. D.** (2003). The molecular motor toolbox for intracellular transport. *Cell* **112**, 467–480.
- Vessey, J. P., Vaccani, A., Xie, Y., Dahm, R., Karra, D., Kiebler, M. A. and Macchi, P.** (2006). Dendritic localization of the translational repressor Pumilio 2 and its contribution to dendritic stress granules. *J. Neurosci.* **26**, 6496–6508.
- Voronina, E. and Seydoux, G.** (2010). The *C. elegans* homolog of nucleoporin Nup98 is required for the integrity and function of germline P granules. *Development* **137**, 1441–1450.
- Voronina, E., Paix, A. and Seydoux, G.** (2012). The P granule component PGL-1 promotes the localization and silencing activity of the PUF protein FBF-2 in germline stem cells. *Development* **139**, 3732–3740.
- Weidmann, C. A. and Goldstrohm, A. C.** (2012). *Drosophila* Pumilio protein contains multiple autonomous repression domains that regulate mRNAs independently of Nanos and brain tumor. *Mol. Cell. Biol.* **32**, 527–540.
- Wilkie, G. S. and Davis, I.** (2001). *Drosophila* wingless and pair-rule transcripts localize apically by dynein-mediated transport of RNA particles. *Cell* **105**, 209–219.
- Zhang, B., Gallegos, M., Puoti, A., Durkin, E., Fields, S., Kimble, J. and Wickens, M. P.** (1997). A conserved RNA-binding protein that regulates sexual fates in the *C. elegans* hermaphrodite germ line. *Nature* **390**, 477–484.